Biophysical Journal, Volume 96

Supporting Material

The 3-Dimensional Dynamics of Actin Waves, a Model of Cytoskeletal Self-organization

Till Bretschneider, Kurt Anderson, Mary Ecke, Annette Müller-Taubenberger, Britta Schroth-Diez, Hellen C. Ishikawa-Ankerhold, and Günther Gerisch

Supplemental Data
The 3-Dimensional Dynamics of Actin Waves, a Model of Cytoskeletal Self-organization

Till Bretschneider, Kurt Anderson, Mary Ecke, Annette Müller-Taubenberger, Britta Schroth-Diez, Hellen C. Ishikawa-Ankerhold, and Günther Gerisch

Supplemental Experimental Procedures

Vector constructs for expression of fluorescently tagged proteins in *Dictyostelium*

The endogenous *Dictyostelium* proteins fused to green fluorescent protein (GFP S65T), enhanced monomeric red fluorescent protein [mRFPmars (7)], or DdmCherry are expressed under control of the actin-15 promoter. Vector constructs for GFP-coronin (20), GFP-actin (S1), GFP-Arp3 (S2), LimEΔ-GFP (4), and mRFPmars-LimEΔ (7) are based on the *Dictyostelium* pDEXRH vector, which is stably integrated into the genome (S3). For DdmCherry, the cDNA sequence encoding mCherry (S4) was adapted to the codon usage of *Dictyostelium* and synthesized as described (S5). The DdmCherry sequence contains one amino-acid exchange (E33K) compared to the original mCherry. The DdmCherry DNA was cloned into pBsrH-GFP (S6) via *Hin*dIII and *Eco*RI by replacing the GFP sequence. Subsequently LimEΔ was cloned into this vector via *Eco*RI.

For construction of the vector encoding GFP-CARMIL, the coding sequence of CARMIL was amplified by PCR using AX2 genomic DNA as template, and was cloned into pBsrH-GFP via *Eco*RI. GFP-MyoB is encoded by an extrachromosomal vector kindly provided by Margaret Titus, University of Minnesota.

Culture conditions and transformation of *Dictyostelium* cells

Cells of *Dictyostelium discoideum* strains were cultivated at 23±2°C in nutrient medium on polystyrol Petri dishes. If not stated otherwise, AX2-214 cells were used for transformation with plasmids enabling the expression of fluorescent fusion proteins. The cells were chilled, washed twice with ice-cold 17 mM K-Na-phosphate buffer, pH 6.0, and electroporated using a Bio-Rad gene pulser at 0.8-1.0 kV and 3 µF with 4-mm cuvettes. After 24 h, 10 µg of blasticidin-S (ICN Biomedicals Inc., Costa Mesa, CA, USA) or 5 to 20 µg of geneticin (G418; Sigma Corp.) per ml were added for selection. In the AX2-derived gene disruption mutant HS2205 lacking myosin-II heavy chains (24), mRFP-LimEΔ was expressed using G418 for selection. In the Gβ-null mutant LW6 and its parent DH1 (27), LimEΔ-GFP was expressed using G418 for selection. SCAR-null mutant cells derived from the *D. discoideum* strain AX3 (31) were kindly provided by Robert Insall, Beatson Institute for Cancer Research, Glasgow (UK), and transfected to express GFP-Arp3 and Cherry-LimEΔ using for selection G418 or blasticidin, respectively. Transformants were cloned on lawns of *E. coli* B/2, and those showing expression of fluorescent proteins were selected for further analysis.

For studying the localization of GFP and mRFP fusion proteins, cells were washed twice in 17 mM K-Na-phosphate buffer, pH 6.0, and were transferred to a glass coverslip in an open chamber.

Fluorescent labeling and live-cell imaging

To visualize actin waves simultaneously with associated proteins, it was necessary to acquire dual-fluorescence images of high spatial resolution at the sub-second time scale with a minimum of irradiation damage and photobleaching. We have imaged pairs of proteins expressed in the same cells, one tagged with GFP, the other with either mRFP or mCherry. To visualize actin, two probes were applied. GFP-actin (S1) caused a high background due to unpolymerized GFP-actin in the cytoplasm. The lowest background was obtained by labeling the actin filament system with a truncated LimE construct (LimEΔ) that lacks the C-terminal coiled-coil domain of the protein (4). GFP-tagged MyoB has previously been used to localize this motor protein at the membrane of rocketing phagosomes (50). GFP-tagged Arp3, a subunit of the Arp2/3 complex, has been used to study recruitment of the complex to leading edges, phagocytic cups, and other dynamic structures of the actin cortex (4, 51).

For 3-D reconstructions, z-stacks were obtained at 200 nm distances using a Nikon Eclipse TE300 microscope equipped with a 100x/1.4 oil Plan Apo objective, a Perkin Elmer Ultra View spinning disc scanner and a Hamamatsu Photonics ORCA-ER, model C4742-95-12-ERG camera. GFP and mRFP emissions were separated using alternately a 488 nm/525 ±50 nm and a 568 nm/700 ±75 nm filter set. Deconvolution was performed using Huygens Essential from SVI (Hilversum, The Netherlands) with the Nipkow Disc Option. The calculation was based on a theoretical point spread function, assuming a refractory index of 1.37 for the cytoplasm of *Dictyostelium* (S7), combined with maximum likelihood estimation.

Images were processed using ImageJ software (**http://rsb.info.nih.gov/ij/**) with customized macros and plugins.

Dual-color TIRF microscopy

For TIRF microscopy a “through-the-objective” setup was employed using standard coverslips and conventional immersion oil. An Olympus 100x/1.45 NA objective on an IX-71 inverted microscope with a custom built condensor (VisiTirf, designed in conjunction with Visitron GmbH, 82178 Puchheim, Germany) was used. For GFP and mRFP, light from an Innova 70C Kr-Ar mixed gas laser (Coherent, Dieburg Germany) was passed through an Opto-Electronique AOTF (supplied by Visitech, Sunderland, UK) to select and modulate the power of the 488 and 568 nm lines for fluorescent protein excitation. If possible, both GFP and mRFP were excited at 488 nm to insure excitation to the same depth within the sample. For 488 or 491 nm excitation alone the filter cube contained a 488/10 laser clean up filter in the excitation position, a z488rdc dichroic, and a 500LP emission filter. For dual excitation at 488 nm and 568 nm the cube contained a 488/568 dual laser clean up filter in the excitation position, a 51006bs double bandpass dichroic, and no emission filter. Red and green channels were imaged simultaneously using a Dual-View emission splitter (Optical Insights, supplied by Visitron) inserted between the microscope body and the camera, which contained a 525/50 filter in the green channel, a 630/60 filter in the red channel, and a 595 nm dichroic to split red from green. Images were acquired using a Princeton Instruments MicroMax 512 EBFT camera driven by MetaMorph software (both supplied by Visitron). For merged images the two channels were adjusted with a tolerance of 1 to 2 pixels.

For GFP and mCherry (Fig. 6 and movies 13 and 14), the system was equipped with a two-line Andor laser combiner (ALC, Andor Technology, Belfast, Northern Ireland) housing a Cobolt Calypso (491 nm, 75 mW) and a Cobolt Jive (561 nm, 75 mW; Cobolt AB, Solna, Sweden) solid-state laser, an AOTF and an Andor PCU100 control unit. Red and green channels were imaged concurrently using an OptoSplit image splitter (Cairn Research Ltd., Kent, UK; equipped with a 565 DCXD dichroic, and BrightLine HC 525/30 and HC 628/40 emission filters.

All filters were from Chroma, Rockinham, VT, USA, or Semrock, Rochester, NY, USA; supplied by AHF Analysentechnik, 72005 Tübingen, Germany. Images were acquired using an Andor iXon+DU897_BV (Andor) EM-CCD camera controlled by IQ 1.8 software. For the large image of Figure 6 the channels were fit to each other using red/green fluorescent beads and the program www.kalaimoscope.com (S8) for correction.

Photobleaching and recording of fluorescence recovery

FRAP was performed using an Olympus FV-1000 laser scanning confocal microscope with a 405 nm laser coupled through the simultaneous scanning port. This microscope configuration had two separate pairs of X- and Y-scanning mirrors which allowed image data to be continuously acquired using 488-nm excitation while a small region of the sample was independently photobleached using a 405-nm laser. The image acquisition rate was 64 ms per frame, with 500 ms of data acquisition prior to a 120 ms (i.e. approximately 2 frames) photobleach event. Photobleaching was performed using the 'cyclone' bleach function, in which the laser starts in the middle of a circle and processes outward in a spiral pattern. Bleach size was 20 pixels (approximately 2 microns in diameter). The time and intensity of photobleaching were selected to achieve greater than 75% signal reduction in the selected region. Scanning was performed at zoom 8 (0.103 microns per pixel) using an NA 1.1 PLAPO 60x OLSM objective in 12 bit acquisition mode. GFP was imaged over a 500-550 nm and mRFP over a 600-660 nm emission range. Care was taken to minimize saturated pixels in the acquired images. The profile of the bleached area was determined by bleaching a fluorescent plastic slide (Chroma).

Supplemental References

(S1) Westphal, M., Jungbluth, A., Heidecker, M., Mühlbauer, B., Heizer, C., Schwartz, J.-M., Marriott, G., and Gerisch, G. (1997). Microfilament dynamics during cell movement and chemotaxis monitored using a GFP-actin fusion protein. Curr. Biol. 7, 176-183.

(S2) Insall, R., Müller-Taubenberger, A., Machesky, L., Köhler, J., Simmeth, E., Atkinson, S.J., Weber, I., and Gerisch, G. (2001). Dynamics of the *Dictyostelium* Arp2/3 complex in endocytosis, cytokinesis, and chemotaxis. Cell Motil. Cytoskel. 50, 115-128.

(S3) Faix, J., Gerisch, G., and Noegel, A.A. (1992). Overexpression of the csA cell adhesion molecule under its own cAMP-regulated promoter impairs morphogenesis in *Dictyostelium*. J. Cell Sci. 102, 203-214.

(S4) Shaner, N.C., Campbell, R.E., Steinbach, P.A., Giepmans, B.N., Palmer, A.E., Tsien, R.Y. (2004). Improved monomeric red, orange and yellow fluorescent proteins derived from *Discosoma* sp. red fluorescent protein. Nat. Biotechnol. 22, 1567-1572.

(S5) Fischer, M., Haase, I., Wiesner, S., and A. Müller-Taubenberger. 2006. Visualizing cytoskeleton dynamics in mammalian cells using a humanized variant of monomeric red fluorescent protein. FEBS Lett. 580, 2495-2502.

(S6) Müller-Taubenberger, A. (2006). Application of fluorescent protein tags as reporters in life cell imaging studies. In: *Dictyostelium discoideum* Protocols (eds. L. Eichinger and F. Rivero-Crespo), Humana Press. Methods Mol. Biol. 346, 229-246.

(S7) Gingell, D., and Todd, I. (1979). Interference reflection microscopy: a quantitative theory for image interpretation and its application to cell-substratum separation measurement. Biophys. J. 26, 507-526.

(S8) Rink, J., Ghiko, E., Kalaidzidis, Y.L., and Zerial, M. (2005). Rab conversion as a mechanism of progression from early to late endosomes. Cell 122, 735-749.

Supplemental Figure 1.
Unprocessed images of the z-stacks that are shown in Figure 8A after deconvolution. Numbers and directions of the scans are the same as in Figure 8.

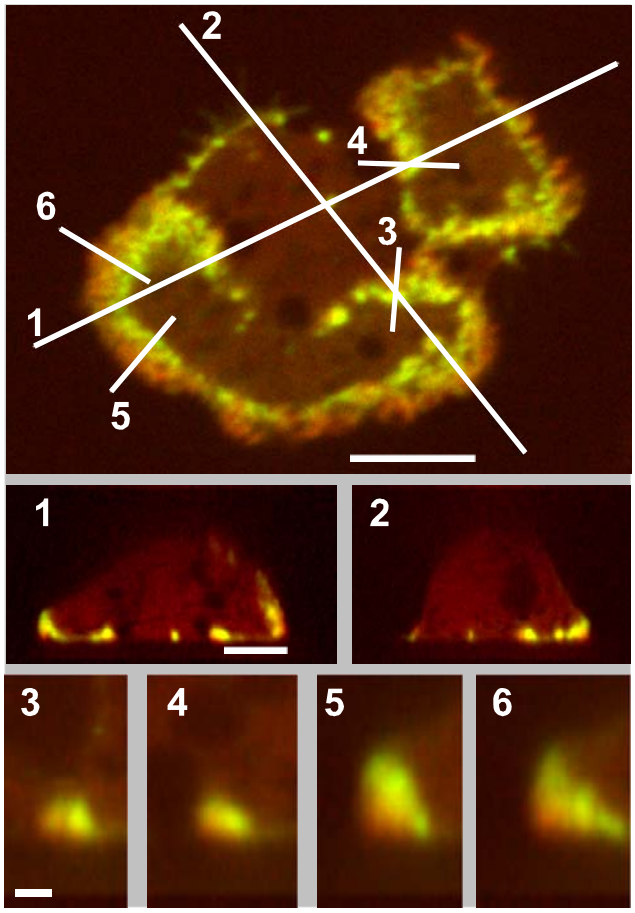

Movies

All movies show TIRF images. In merged images of double-labeled cells, the actin label is shown in red and the respective GFP-labeled protein in green.

Movie 1. Cell labeled with GFP-Arp3 and mRFP-LimEΔ. Early during recovery of actin polymerization after the removal of latA, mobile patches are formed that are enriched in both filamentous actin and the Arp2/3 complex (yellow areas where the two labels are merged). Subsequently, a wave is formed, which expands, collapses, and changes its position on the substrate-attached cell surface. Frame-to-frame interval 1 s. Bar, 5 μm.

Movie 2. Cell labeled with GFP-Arp3 and mRFP-LimEΔ. In this collapsing wave, trails enriched in the Arp2/3 label are left behind actin-enriched structures. Frame-to frame interval 1 s. Bar, 5 μm.

Movie 3. Cell shown in figure 1B, labeled with GFP-Arp3 and mRFP-LimEΔ. In this wave a patchwork of green, yellow, and red spots is especially clear, indicating varying ratios of Arp2/3 and actin in these sub-structures of the wave. Frame-to-frame interval 1 s. Bar, 5 μm.

Movie 4. Wave formation in cells lacking myosin-II heavy chains. Four short sequences are compiled that show waves labeled with mRFP-LimEΔ. The first three sequences illustrate retracting waves. The last sequence shows in the middle a cell with two waves, one of which is splitting into two. Actin patches outside the wave area are mostly involved in clathrin-dependent endocytosis (51). Frame-to frame internal 1 s. Bar, 10 μm.

Movie 5. Cell labeled with GFP-MyoB and mRFP-LimEΔ. The expanding and collapsing wave shows MyoB primarily at the front of actin structures. Frame-to-frame interval 1 s. Bar, 5 μm.

Movie 6. Cell labeled with GFP-MyoB and mRFP-LimEΔ, showing wave pattern with independently moving arrays of actin headed by MyoB. Frame-to-frame interval 1 s. Bar, 5 μm.

Movie 7. Wave dynamics in a cell expressing GFP-CARMIL and mRFP-Lim-EΔ.The wave retracts, splits into multiple waves, and expands repeatedly. Frame-to-frame interval 2 s. Bar, 10 μm.

Movie 8. Reversal of wave direction in the cell shown in Figure 3, labeled with GFP-CARMIL and mRFP-LimEΔ. Here fluorescence emission in the GFP-CARMIL channel is shown separately. Frame-to frame interval 0.5 s. Bar, 10 μm.

Movie 9. Cell labeled with GFP-coronin and mRFP-LimEΔ. Two waves are fusing when two areas of cell-substrate contact unite. The actin zone is followed by a coronin-enriched band. Frame-to-frame interval 2 s. Bar, 10 μm.

Movie 10. Cell labeled with GFP-coronin and mRFP-LimEΔ. During expansion, collapsing, and splitting into two or three waves, the coronin-enriched zones always follow the actin fronts. Frame-to-frame interval 2 s. Bar, 10 μm.

Movie 11. Wave dynamics in a Gβ-null cell. The cell is labeled with LimEΔ-GFP. Frame-to-frame interval 1 s. Bar, 10 μm.

Movie 12. Waves and actin network structure in a Gβ-null cell. The cell labeled with LimEΔ-GFP shows two extensively expanding waves. During their retraction, the actin network outside the wave becomes clearly visible. Frame-to-frame interval 1 s. Bar, 10 μm.

Movie 13. Wave propagation and Arp3 recruitment without SCAR. The same wave as in Figure 6 is shown, with the Cherry-LimEΔ label for actin in the left-hand panel, and the GFP-Arp3 in the right panel. Frame-to-frame interval 1 s. Bar, 10 μm.

Movie 14. Actin and Arp3 in a SCAR-null cell. Similar as in movie 13, an extensively expanding wave is formed. Initiation of this wave is preceded by 6 minutes of fluctuating actin and Arp3 accumulations that do not expand into a circular wave (only about half of this phase is shown). Frame-to-frame interval 1 s. Bar, 10 μm.